Cement and Concrete Research 41 (2011) 932–941

Contents lists available at ScienceDirect

Cement and Concrete Research

journal homepage: http://ees.elsevier.com/CEMCON/default.asp

Rheology and vibration of fresh concrete: Predicting the radius of action of poker vibrators from wave propagation

P.F.G. Banfill *, M.A.O.M. Teixeira, R.J.M. Craik

School of the Built Environment, Heriot-Watt University, Edinburgh, EH14 4AS, UK

ARTICLE INFO

Article history:
Received 17 January 2011
Accepted 22 April 2011

Keywords:
Fresh concrete (A)
Vibration (A)
Bingham model
Rheology (A)

ABSTRACT

The compaction of fresh concrete by an internal poker vibrator has been analysed using closed-form solutions for the propagation of the shear and compressive waveforms, assuming that concrete conforms to the Bingham model. In the inner liquefied zone around the vibrator the flow is due to shear whereas in the outer unsheared zone propagation is due to compressive waves. The analysis gives a method of predicting the radial position at which the flow changes, which coincides with the radius of action of the vibrator. Theory and experiment agree well and confirm that the peak velocity of the vibration governs its efficacy, with radius of action increasing with increasing velocity. The radius of action increases with decreasing yield stress and with increasing plastic viscosity. The work offers the potential to optimise the design and use of vibrators.

1. Introduction

For decades it has been worldwide industrial practice to use vibration to compact fresh concrete into formwork and around reinforcement, releasing air bubbles and producing concrete of the highest density, strength and durability [1]. Even with the increasing utilization of self-compacting concrete, vibrators are still in widespread use, so it is justifiable to seek improvements in the efficiency of the vibration process. This paper presents a new analysis of the behaviour of concrete under the action of immersed internal vibrators which has the potential to deliver those improvements.

2. Previous work

It has long been known that fresh concrete conforms to the Bingham model [2], confirmed by the ordinary everyday observation that it can stand unsupported without flowing under its own weight (as in the slump test). This model can be expressed as:

$$\tau = \tau_0 + \mu\dot{\gamma} \quad (1)$$

where concrete can support shear stresses $\tau<\tau_0$, the yield stress, without flowing (i.e. shear rate $\dot{\gamma}=0$) but flows at higher stresses. In common with all yield stress materials fresh concrete is a weak solid below the yield stress while above the yield stress it flows as a liquid with a plastic viscosity μ.

Phenomenologically, vibration appears to remove or overcome the yield stress of concrete, which then flows under its own weight. The phenomena have been described empirically and there is an extensive literature on the role of frequency, amplitude and acceleration of the imposed vibration on its efficacy [1], but in most cases the characteristics of the concrete have taken second place in importance to those of the vibration. In research reports and practical guidelines workability has generally been defined in terms of single point tests, which, as has been pointed out before, are fundamentally incapable of reliably distinguishing different concretes [2]. Tattersall and Baker were the first to attempt to relate the rheology of fresh concrete to its behaviour under vibration. They used an electromagnetic vibrating table as a well-characterised source and found that the governing characteristic of the vibration is its peak velocity [3,4]. They showed that the fluidity of vibrated concrete, defined as the reciprocal of its low shear rate viscosity, is proportional to peak vibrational velocity up to a critical value, above which it remains constant. With fresh concretes of different rheological characteristics the viscosity of the vibrated concrete is proportional to the plastic viscosity of the unvibrated concrete [5].

When an internal poker vibrator is used there is a clearly visible liquefied region near the vibrator, from which air bubbles are released, while at greater distances the concrete seems unaffected. The radius of action of the vibrator is a parameter of considerable practical importance which governs the productivity with which concrete can be compacted. Many empirical studies on the effects of internal vibrators on fresh concrete have been reported [6–9] but knowledge of the theory and controlling mechanisms for the flow around a vibrator is limited. Taylor [9] investigated the influence of frequency and amplitude on the efficacy of internal vibrators, as shown by the radius of action within which the vibrator was capable of compacting the concrete to 2% air content, as determined by gamma ray attenuation in the hardened concrete. He found that the efficacy is influenced by frequency f and amplitude A and that for a given acceleration ($\propto f^2A$), a

* Corresponding author. Tel.: +44 131 451 4648; fax: +44 131 451 3161.
E-mail address: p.f.g.banfill@hw.ac.uk (P.F.G. Banfill).

0008-8846/$ – see front matter © 2011 Elsevier Ltd. All rights reserved.
doi:10.1016/j.cemconres.2011.04.011

vibrator with high amplitude is more effective than one with low amplitude but higher frequency. This is consistent with the peak velocity criterion ($\propto fA$) mentioned above, as shown by the following example. Consider a vibrator of amplitude 0.5 mm and frequency 100 Hz. To maintain a constant acceleration when the amplitude is doubled to 1 mm the frequency must drop to 70.7 Hz, but in so doing the velocity increases by a factor of √2 and the vibrator is seen to be more effective. Similarly, to maintain a constant acceleration when the amplitude is halved to 0.25 mm the frequency must rise to 141.4 Hz, but in doing so the velocity is reduced by a factor of √2 and the vibrator is consequently less effective.

Asserting that the radius of action is due to attenuation, ACI Committee 309's state-of-the-art review [1] recommends a formula first presented by Dessoff in 1937 [10] for estimating the geometrical energy distribution due to the radial generation of compressive waves around an internal vibrator:

$$u_r = u_o\sqrt{\frac{r_i}{r}\exp\left[-\frac{\Omega}{2}(r-r_i)\right]} \tag{2}$$

where u_r is the radial velocity at radius r, u_o is the velocity of vibration of the vibrator surface and r_i its radius. Ω is the coefficient of damping, and for concrete of consistency ranging from flowing to plastic, a value of between 0.04 and 0.08 is suggested [1]. Dessoff's formula was originally presented as an approximate procedure for the study of compact soil, and its application to concrete can be criticised on the grounds that compressive waves do not propagate through liquids, and therefore its use would be restricted to the outer region where the concrete is not liquid, a restriction that is not mentioned by ACI Committee 309. The damping is due to internal friction between the solid particles (1). If the formula is not applicable to the liquid region surrounding the vibrator a new approach based on shear wave propagation is needed. Teixeira et al. [11] presented a preliminary analysis in terms of the propagation of shear waveforms outward from the surface of the vibrator. The amplitude of the wave decays with distance and at a critical distance has fallen to a level that is insufficient to exceed the yield stress. Beyond this distance the concrete is solid and in this region the motion is controlled by the compressive waveforms. This critical point corresponds to the radius of action of the vibrator and this paper develops this alternative analysis of wave propagation in the two regions.

The main objective of this paper is therefore to analyse the radius of action of vibrators in relation to the rheology of the fresh concrete and the characteristics of the vibration. A subsidiary objective is to investigate the possibility that the decay of acceleration in the liquid region is simply a consequence of the shear wave propagation.

3. Theory

3.1. Problem definition and research approach

In the proposed approach, the vibrational process for a poker vibrator in fresh concrete is analysed as two distinct cases, namely: (i) the oscillating two-dimensional incompressible viscous fluid motion around a cylinder in a confining volume of material, i.e. a shear waveform, and (ii) the acoustic motion of a cylindrical travelling wave with dissipation of energy, i.e. a compressive waveform. The theoretical analysis is also investigated experimentally and a prediction approach is developed.

The construction of a poker-type internal vibrator for concrete is shown schematically in Fig. 1. An eccentric mass inside a fixed cylindrical casing of radius r_i rotates about the point O and makes the casing oscillate. The entire assembly moves in such a way that a point P on the surface of the casing describes a circular path of a radius that is small compared to r_i but the casing itself does not rotate. During operation, at any instant t, point P imparts to the surrounding medium

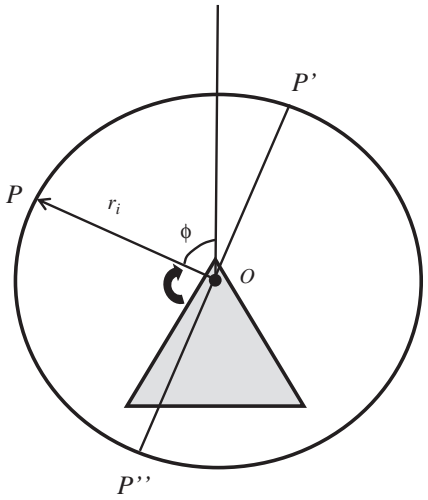

Fig. 1. Construction of a poker type vibrator.

a compressive force in the direction φ, while points P' and P'', at angles $\varphi \pm \pi/2$, impart a shear force in the directions $\pm\varphi$. Since a compressive waveform cannot propagate through a liquid medium only the shear excitation needs to be considered.

3.2. Shear waveform

Alexander [12] studied the mechanics of motion of fresh concrete during vibration using a mechanical driving point impedance technique. He found different mechanical impedance curves depending on whether the dynamic stress applied is above or below a threshold level, i.e. the yield stress, although he did not call it this. Fresh concrete below the yield stress possesses the mass, damping and stiffness characteristics of a solid, while above the yield stress it is a liquid. Various combinations of force and frequency were found to cause liquefaction, which was associated with a simultaneous sharp drop in impedance. His experimental results showed that concretes of normal consistencies behave like a fluid during vibration, as confirmed by the results of Tattersall and Baker [3,4] and Banfill et al. [5]. Therefore the use of hydrodynamic theory to analyse the liquefaction process is justified.

Chen et al. [13] presented an analytical and experimental study of a cylindrical rod vibrating in a viscous liquid enclosed by a rigid concentric cylindrical shell. Fig. 2 shows the coordinate system they used and the vibrator casing is represented by an infinitely long cylinder of radius r_i oscillating with velocities:

$$u_r = u_0\cos\theta(\cos\omega t + i\sin\omega t) \text{ and } u_\theta = -u_0\sin\theta(\cos\omega t + i\sin\omega t) \tag{3}$$

where u_r and u_θ are the velocity components in the radial and tangential directions at an arbitrary point on the casing which subtends an angle θ to the coordinate axis, $i^2 = -1$, $\omega = 2\pi f$ is the angular velocity, u_0 is the peak velocity and f is the frequency. Where the amplitude of oscillation of the source is small compared to its dimensions, the equations for the conservation of mass and momentum may be linearised [14] as:

$$\nabla^4\psi - \frac{1}{\nu}\frac{\partial}{\partial t}\nabla^2\psi = 0 \tag{4}$$

where ψ is the stream function, ∇^2 is the Laplacian operator and ν is the kinematic viscosity of the fluid. This assumption is reasonable for most internal vibrators, for which the amplitude is less than 1 mm and r_i is typically 25 mm. The velocity components for the fluid are given

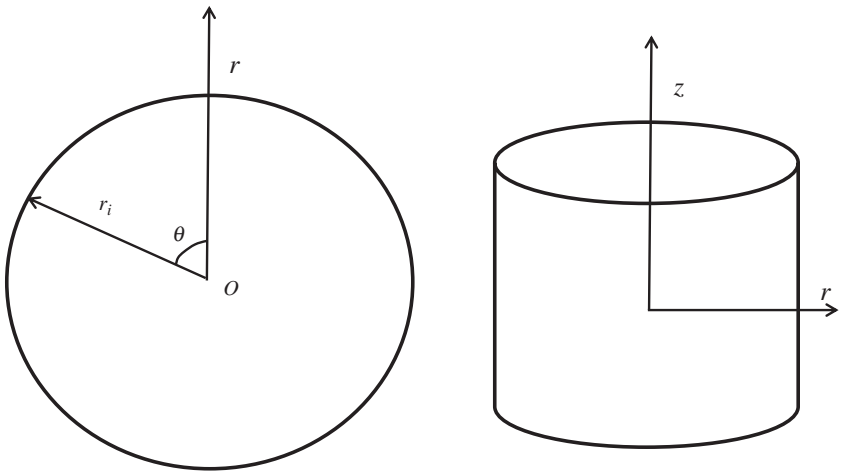

Fig. 2. The coordinate system used in the equations.

by:

$$u_r = -\frac{\partial\psi}{r\partial\theta} \qquad \text{and} \quad u_\theta = \frac{\partial\psi}{\partial r} \tag{5}$$

giving the solution of Eq. (4) as:

$$\psi = u_o\left[A\left(\frac{r_i^2}{r}\right) + Br + Cr_iI_1(kt) + Dr_iK_1(kr)\right]\sin\theta\ \exp(i\omega t) \tag{6}$$

where

$$k = \sqrt{i\frac{\omega}{\nu}}.$$

A, B, C, D are arbitrary constants that can be determined as [13]:

$$A = \left\{-\alpha^2[I_0(\alpha)K_0(\beta) - I_0(\beta)K_0(\alpha)] + 2\alpha[I_1(\alpha)K_0(\beta) + I_0(\beta)K_1(\alpha)]\right\} - 2\alpha\delta[I_0(\alpha)K_1(\beta) + I_1(\beta)K_0(\alpha)] + 4\delta[I_1(\alpha)K_1(\beta) - I_1(\beta)K_1(\alpha)]\} / \Delta \tag{7}$$

$$B = \left\{2\alpha\delta[I_1(\alpha)K_0(\beta) - I_0(\beta)K_1(\beta)] + \alpha^2\delta^2[I_0(\alpha)K_0(\beta) - I_0(\beta)K_0(\alpha)] - 2\alpha\delta^2[I_1(\alpha)K_0(\beta) + I_0(\beta)K_1(\alpha)]\right\} / \Delta \tag{8}$$

$$C = \left\{-2\alpha K_0(\beta) - 4\delta K_1(\beta) + \delta^2[2\alpha K_0(\alpha) + 4K_1(\alpha)]\right\} / \Delta \tag{9}$$

$$D = \left\{-2\alpha I_0(\beta) + 4\delta I_1(\beta) + \delta^2[2\alpha I_0(\alpha) - 4I_1(\alpha)]\right\} / \Delta \tag{10}$$

where

$$\alpha = kr_i$$

$$\beta = kr_o$$

$$\delta = r_i / r_o$$

and

$$\Delta = \alpha^2\left(1-\delta^2\right)[I_0(\alpha)K_0(\beta) - I_0(\beta)K_0(\alpha)] + 2\alpha\delta\left[I_0(\alpha)K_1(\beta) - I_1(\beta)K_0(\alpha) + I_1(\beta)K_0(\alpha) - I_0(\beta)K_1(\beta)\right] + 2\alpha\delta^2[I_0(\beta)K_1(\alpha) - I_0(\alpha)K_1(\alpha) + I_1(\alpha)K_0(\beta) - I_1(\alpha)K_0(\alpha)]. \tag{11}$$

I_0 and I_1 are modified Bessel functions of the first kind and K_0 and K_1 are modified Bessel functions of the second kind.

Eqs. (5) and (6) can be used to calculate the velocity components in the radial and tangential directions as a function of distance from the source and this can be used to predict the decay of vibration within the inner flow region.

3.3. Compressive waveform

Beyond the critical distance where the amplitude of the oscillatory shear has decreased to the point where the shear stress is less than the yield stress the concrete is unsheared. In this outer region where the effects of vibration are not sufficient to liquefy the Bingham material, the principles of hydrodynamics are no longer applicable. Here fresh concrete behaves as an elastic solid and instead structural vibration theory can be used to describe the motion.

A complete description of the compressive wave motion in a Bingham material at stresses below the yield stress is not available and a simplified first order equation of motion is adopted in this analysis. Assuming that a cylindrical wave spreads outwards from the radial position of the interface between liquid and solid zones, r_{ls}, the amplitude depends only on the radial distance r and the wave equation in cylindrical coordinates for this case is [15]:

$$\frac{1}{r}\frac{\partial}{\partial r}\left(r\frac{\partial u_r}{\partial r}\right) = \frac{1}{c^2}\frac{\partial^2 u_r}{\partial t^2} \tag{12}$$

where u_r is the particle velocity component in the radial direction, c is the velocity of propagation of compressive waves in the material and t is time.

If r_{ls} is small compared to the wavelength the particle velocity component in the radial direction at large distances r is given by [15]:

$$u_r = u_{ls}\pi r_{ls}\sqrt{\frac{f}{cr}}\ \exp\left[i\frac{\omega}{c}(r-ct) - i\left(\frac{\pi}{4}\right)\right] \tag{13}$$

where u_{ls} is the velocity of oscillation at the interface between liquid and solid zones. The assumption that r_{ls} is small compared to the wavelength is reasonable because the velocity of wave propagation in fresh concrete is approximately 500 m/s and the wavelength at a typical vibrator frequency of 200 Hz is therefore 2.5 m, which is sufficiently greater than the typically observed radius of action of an internal vibrator of about 0.2 m. Thus Eq. (13) can be used to calculate the velocity distribution as a function of distance from the source and to predict the decay of vibration outside the liquid region where the Bingham materials behaves as a solid.

Since the vibrational velocity is of interest the ratio of the velocity at any point r to that at the interface between solid and liquid is given by:

$$\frac{u_r}{u_{ls}} = \pi r_{ls}\sqrt{\frac{f}{cr}}. \tag{14}$$

It should be noted that the radial position of the interface is not known *a priori* and therefore the calculations presented here are based on reference values obtained experimentally for u and r that were well inside the solid region beyond the interface. Eq. (14) describes the motion in the solid region and any value of u_{ls} can be used to generate a curve of u_r as a function of distance.

3.4. Radius of action

By definition, the radius of action of the vibrator is the radial position of the interface between the liquid and solid regions r_{ls}. Referring to Fig. 3, at all radii r where $r_i<r<r_{ls}$ the concrete is fluidified and the radius of action defines the size of the fully compacted region. Since there can be no consolidation in the solid region the radius of action cannot be larger than the position of the interface between the two zones, but in practice it may appear somewhat smaller if the shear waveform is decaying only slowly as it approaches the interface. Based on the preceding analysis of the shear and compressive waveforms, it is expected that a radial distribution of velocity will show two zones. The velocity will decrease relatively rapidly with increasing radius through the liquid zone as far as the interface, beyond which it will decrease more slowly with radius into the solid zone. In principle, the point where the two curves cross coincides with the interface between liquid and solid regions and defines the radius of action.

In the liquefied zone the concrete is confined between two concentric cylinders (the vibrator and the unsheared concrete) so the shear stress at radius r decreases from a maximum value τ_w at the surface of the vibrator, radius r_i, to the yield stress τ_0 at the interface between solid and liquid. This is the radius of action and is given by:

$$r_{ls} = \sqrt{\frac{\tau_w}{\tau_0} r_i^2}. \tag{15}$$

The shear stress at the surface of the vibrator τ_w is given by the Bingham model (Eq. (1)):

$$\tau_w = \tau_0 + \mu\dot{\gamma}_w \tag{16}$$

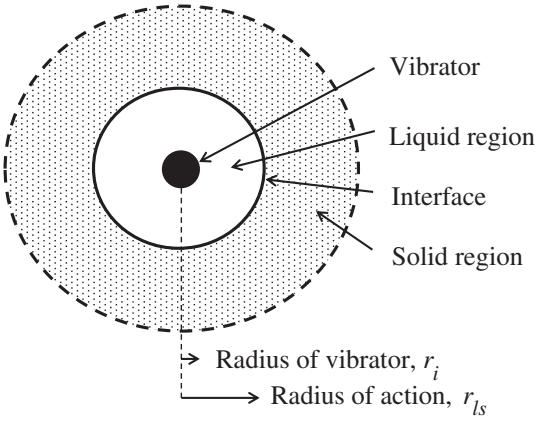

Fig. 3. Definition of the radius of action of a vibrator.

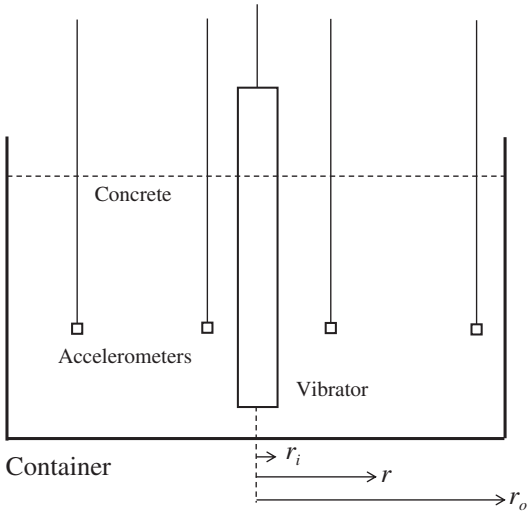

Fig. 4. Experimental set-up for vibration tests.

where τ_0 and μ are the yield stress and plastic viscosity of the concrete, respectively, and the shear rate at the surface of the vibrator $\dot{\gamma}_w$ is given by:

$$\dot{\gamma}_w = r\frac{\partial}{\partial r}\left(\frac{u_\theta}{r}\right) + \frac{1}{r}\frac{\partial u_r}{\partial \theta} \tag{17}$$

where u_r and u_θ may be calculated using Eqs. (4) and (6). With this analysis it becomes possible to predict the radius of action from a knowledge of the characteristics of the vibrator and the rheology of the concrete.

4. Experimental work

The aim of the experimental work was to investigate the applicability of the prediction equations to the practical situation of an internal vibrator immersed in fresh concrete and to identify the liquid and solid zones and the radius of action.

All experimental work was carried out using an electrically driven vibrator (Rotopoka, Fyne Machinery and Engineering Ltd, London) of 28 mm external diameter. Vibrational measurements used piezoelectric accelerometers (Bruel & Kjaer Type 4344), calibrated with a vibration calibrator (Bruel & Kjaer Type 4294), driven by charge amplifiers (Bruel & Kjaer Type 2635) and analysed with a dual channel frequency analyser (Bruel & Kjaer Type 2032). The acceleration levels in the radial, tangential and axial directions were measured at different positions along the vibrator, as well as the magnitude and phase difference between the radial and tangential acceleration levels. The accelerometer was attached to the vibrator with a $20\times20\times40$ mm aluminium block held in place by a circular screw clip. In all tests the vibrator was fully immersed in the fresh concrete sample in order to prevent overheating, as recommended by the manufacturer, and the vibrator and its attached accelerometer were removed from the concrete before it had a chance to set and thoroughly cleaned.

Measurements in fresh concrete were carried out in the apparatus shown schematically in Fig. 4. Accelerometers capable of measuring the acceleration in radial, tangential and axial directions were immersed at 25 mm increments of distance from the vibrator. Two containers were used: (1) a steel cylinder 640 mm internal diameter and 400 mm high, closed at the bottom and (2) a cuboidal timber mould 1500×1500 mm and 500 mm high. Container 1 was a compromise between the need to be larger in diameter than the anticipated size of the zone of liquefaction and the capacity of the concrete mixer available in the laboratory. Container 2 was much

larger so as to avoid any possible interference of the walls of the mould with wave propagation. In each case the vibrator was held vertically in the centre of the container by a frame.

Two ordinary concretes were used in the tests and one further concrete was used for predictions of the radius of action. Concrete A was prepared in a 0.2 m^3 laboratory pan mixer and was used in the smaller container 1. Concrete B was obtained from a ready-mixed concrete supplier and was used in the much larger container 2. Concrete C was prepared in a 0.2 m^3 laboratory pan mixer with the sole purpose of providing the rheological data upon which the predictions of radius of action could be made for comparison with Taylor's results [9]. All concretes used aggregate of maximum particle size 20 mm but unfortunately details of the mixture proportions have been lost. The concretes were characterised by the slump test and the two-point workability test, using the apparatus described by Domone et al. [16]. Density was determined according to BS EN 12350–6 [17]. Velocity of sound was determined for each concrete using a time of flight measurement. Transient plane wave impulses were generated by a frequency analyser (dual channel Bruel & Kjaer Type 2032) and imparted to the fresh concrete by a small shaker/vibrator (LDS Type 406) driven by a power amplifier (Bruel & Kjaer Type 2706) at levels too low to cause liquefaction and detected by an accelerometer (Bruel & Kjaer Type 4500) connected to a storage oscilloscope (Gould type 1421).

5. Results

5.1. Characterisation of concrete

Table 1 summarises the properties of the experimental concretes. Concretes A and B were similar, though not identical, and while of a fairly soft consistency they are representative of concretes that would require vibratory compaction in practice. The lower slump of concrete B is consistent with its higher yield stress but the plastic viscosities were significantly different, as a result of the different constituent materials [2]. The velocity of sound in the fresh concrete is consistent with values reported by other authors who have used shear wave or pulse propagation techniques to monitor setting processes [18]. Concrete C was chosen to be similar to that used in Taylor's investigations [9].

5.2. Characterisation of the vibrator

Tested in free air, the accelerations of the vibrator in the radial and tangential directions were identical, with a phase angle of 90°, confirming that the vibrator performs an oscillatory motion in a circular path. The measured frequency was 246 Hz and the acceleration was 1122 m/s^2 RMS, providing a peak velocity of oscillation $u_o = 1.03$ m/s. The acceleration in the axial direction was negligibly small and can be ignored in comparison to that in the other directions.

5.3. Propagation of vibration

Fig. 5 shows the results for concrete 1 in container A. The symbols represent the measured data and are the average of 10 tests, while the lines show the predictions from the shear and compressive waveform equations. In the liquid zone the radial and tangential velocity components for the shear wave (Eq. (5)) are almost identical. Only the radial velocity is available for the compressive waveform (Eq. (13)). Fig. 5 also shows a curve plotted using Dessoff's equation [1,10] and the predicted value for the radius of action, calculated from Eq. (15). The radius of action was also determined visually from a cross-section cut through the concrete after it had been allowed to harden and found to be approximately 200 mm, in good agreement with the predicted value.

Table 1
Properties of the concrete mixtures.

Concrete	Slump mm	Yield stress Pa	Plastic viscosity Pa s	Plastic density kg/m^3	Sound velocity m/s
A	180	570	15	2300	445
B	150	620	26	2200	515
C	5	2200	150	2200	-

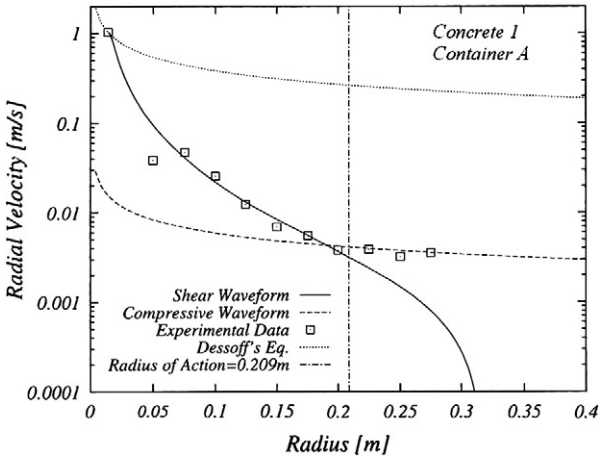

Fig. 5. Radial velocity results for concrete A in container 1.

Fig. 6 presents the results for concrete 2 in container B, where again the symbols represent the measured data and are the mean of three tests, while the lines show the predictions.

5.4. Radius of action

Fig. 7 shows a comparison between the radius of action results determined experimentally by Taylor [9] and those obtained from the prediction method introduced in this paper. Taylor used concrete of very low workability (6 mm slump) but gave no other information on the rheological properties. The prediction values therefore use the properties determined for concrete C (Table 1).

6. Discussion

The experimental results (Fig. 5) show a rapid decay in velocity from the surface value of 1.03 m/s as the distance from the vibrator increased. The experimental velocity distribution in the liquid region

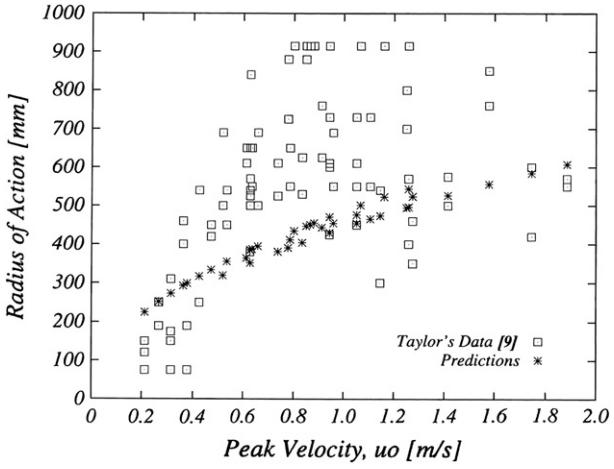

Fig. 6. Radial velocity results for concrete B in container 2.

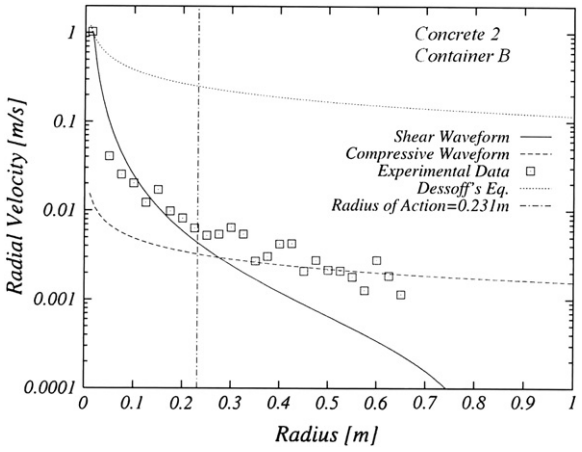

Fig. 7. Effect of peak velocity on the radius of action.

agrees well with the prediction from the shear wave equation as it drops towards the prediction from the compressive wave equation. At a radius of about 0.2 m the shear and compressive curves cross and the experimental points start to follow the upper compressive curve. The excellent agreement between the simple theoretical model and experimental data in the region near the vibrator confirms that concrete behaves as a liquid in this region. Further from the vibrator, outside the liquid region, the decline of the measured velocity is significantly reduced and is in good agreement with the compressive equation, confirming that the concrete behaves as a solid in this region.

Fig. 5 also shows the Dessoff curve (Eq. (2)), which considerably over-estimates the experimental velocity and is unable to account for the rapid decay in velocity near the vibrator. This confirms that it is unsuitable for the liquid region. However, the shape of the curve is very similar to that of Eq. (14) for the solid region but displaced to velocities which are nearly 100-fold higher, which confirms that Dessoff's original formula applies to solid materials.

In Fig. 5 the two curves predicting the shear and compressive waveform velocity distributions intersect at about 200 mm. The predicted value for the radius of action (Eq. (15)) is 209 mm and the value determined experimentally by visual inspection of the compaction visible in a radially cut section through the hardened concrete is 200 ± 10 mm. Clearly the position of the interface between liquid and solid may be represented by the intersection of the curves and it follows that Eq. (15) may be used to predict the radius of action.

The results with the large mould (container B) shown in Fig. 6 reinforce the previous experiments in the cylinder (container A) but are somewhat less clearly defined, perhaps due to inhomogeneities in the larger volume of concrete used in this test. There is again good agreement between experimental and predicted velocity for the shear waveform within the liquid zone and between experimental and predicted compressive wave velocity in the solid zone towards the extremity of the mould but the transition between the curves is less clearly defined by the experimental points. Eq. (15) predicts the radius of action to be 231 mm in this case, whereas the curves intersect at about 300 mm. Again the Dessoff formula considerably over-estimates the velocities.

The effect of velocity on the radius of action, both as measured by Taylor and predicted by Eq. (15), is shown in Fig. 7. Taylor's experiments were performed in wall-shaped moulds 1200 mm long by 200 mm wide and 600 mm high with the vibrator held vertically on the centre line 300 mm from one end. Consequently the results are very scattered, probably due to internal reflections from the mould surfaces and the possibility of assisted propagation along the wall. Additionally, Taylor's concrete had unknown rheology. While the yield stress is correct for a slump of 5 mm, it is impossible to confirm the plastic viscosity. The fact that the experimental points are mostly above the prediction curve suggests that the plastic viscosity of his concrete may be higher than the 150 Pa s assumed in the prediction. This is quite possible since Taylor describes his concrete as very stiff. It should also be pointed out that Taylor's data in Fig. 7 is duplicated: for each value of velocity there is one radius of action from the visual inspection and one from the gamma ray densitometer measurements, and in most cases the former is lower than the latter. The predicted values are given for the corresponding peak velocities, calculated from Taylor's data.

Despite these reservations, the broad trend is a clear increase in the radius of action with increasing peak velocity, as predicted. It confirms Tattersall and Baker's findings that the peak velocity is the most important characteristic of the vibration. Moreover, Taylor's experimental observation that for a given acceleration a vibrator with large amplitude is likely to perform better than one with lower amplitude and higher frequency is confirmed by the predictions. For example, a vibrator of 30 mm radius giving an acceleration of 395 m/s^2 has a radius of action of 273 mm if operated at 200 Hz and 0.25 mm amplitude, compared to a radius of action of 385 mm if operated at 100 Hz and 1.0 mm amplitude.

7. Implications for concrete practice

The prediction equations for the radius of action of an immersed poker vibrator in a given situation require information on both the concrete properties — yield stress, plastic viscosity and density — and the properties of the poker — diameter, frequency, amplitude — as well as the size of the container. The complexity of these seven variables makes it difficult to answer questions like “What is the radius of action in this situation?” or its converse “What conditions are needed to achieve a given radius of action?” and “What concrete should be used for a particular vibrator and size of container?”, and therefore a small computer program (POKER) was written in C++. This requests the user to enter values for yield stress, plastic viscosity, density, poker diameter, frequency and amplitude, and container size and gives the radius of action. The user interface offers a range of preset values for each variable, but these can be over-written with user-selected values if required. The “container size” box offers a “free field” value to deal with the situation where the mould is effectively of infinite size. Radius of action is then calculated using Eq. (15).

Table 2 shows the results of a parametric survey of the effect of each variable on the predicted radius of action of the vibrator, in the form of a 2^7 factorial design using two levels of each variable (one high and one low). The low and high values are: (i) yield stress 250 and 3000 Pa, (ii) plastic viscosity 25 and 200 Pa s, (iii) density 1800 and 2600 kg/m^3, (iv) poker diameter 20 and 80 mm, (v) frequency 50 and 300 Hz, (vi) amplitude 0.5 and 1.0 mm, and (vii) container size 0.5 m and free field. These values represent the extremes that might be encountered in practice. Comparing rows 1–64 with 65–128 shows that container size has an insignificant effect on the radius of action (i.e. less than 0.01 m) between 0.5 m and free field conditions, except for four combinations at low plastic viscosity (compare row 61 with 125 and row 62 with 126). Comparing successive groups of four rows, e.g. rows 1–4 and 5–8, shows that concrete density has an negligible effect on the radius of action (i.e. some differences of 0.01 m), except for four combinations at low plastic viscosity (compare row 57 with 61 and row 58 with 62). All the other variables have a strong effect: radius of action decreases with increasing yield stress but increases with increasing plastic viscosity (except for eight combinations at high density (compare row 29 with row 31, row 30 with 32, row 61 with 63, and row 62 with 64). Radius of action increases with increasing vibrator diameter, increasing frequency and increasing amplitude, although in some cases the increase is small (e.g. compare row 2 with row 34 (amplitude) and with row 82 (frequency)).

Table 2
Parametric survey of the effect of concrete properties and vibrator characteristics on the calculated radius of action of a vibrating poker.

Row No.	Yield stress Pa	Plastic viscosity Pa s	Density kg/m^3	Poker diameter mm	Frequency Hz	Amplitude mm	Container size[a] m	Predicted radius of action m
1	250	25	1800	20	50	0.5	0.5	0.13
2	3000	25	1800	20	50	0.5	0.5	0.04
3	250	200	1800	20	50	0.5	0.5	0.38
4	3000	200	1800	20	50	0.5	0.5	0.11
5	250	25	2600	20	50	0.5	0.5	0.13
6	3000	25	2600	20	50	0.5	0.5	0.04
7	250	200	2600	20	50	0.5	0.5	0.38
8	3000	200	2600	20	50	0.5	0.5	0.11
9	250	25	1800	80	50	0.5	0.5	0.27
10	3000	25	1800	80	50	0.5	0.5	0.09
11	250	200	1800	80	50	0.5	0.5	0.76
12	3000	200	1800	80	50	0.5	0.5	0.22
13	250	25	2600	80	50	0.5	0.5	0.27
14	3000	25	2600	80	50	0.5	0.5	0.09
15	250	200	2600	80	50	0.5	0.5	0.76
16	3000	200	2600	80	50	0.5	0.5	0.22
17	250	25	1800	20	300	0.5	0.5	0.33
18	3000	25	1800	20	300	0.5	0.5	0.1
19	250	200	1800	20	300	0.5	0.5	0.93
20	3000	200	1800	20	300	0.5	0.5	0.27
21	250	25	2600	20	300	0.5	0.5	0.33
22	3000	25	2600	20	300	0.5	0.5	0.1
23	250	200	2600	20	300	0.5	0.5	0.93
24	3000	200	2600	20	300	0.5	0.5	0.27
25	250	25	1800	80	300	0.5	0.5	0.66
26	3000	25	1800	80	300	0.5	0.5	0.19
27	250	200	1800	80	300	0.5	0.5	1.86
28	3000	200	1800	80	300	0.5	0.5	0.54
29	250	25	2600	80	300	0.5	0.5	2.7
30	3000	25	2600	80	300	0.5	0.5	0.78
31	250	200	2600	80	300	0.5	0.5	1.86
32	3000	200	2600	80	300	0.5	0.5	0.54
33	250	25	1800	20	50	1.0	0.5	0.19
34	3000	25	1800	20	50	1.0	0.5	0.06
35	250	200	1800	20	50	1.0	0.5	0.54
36	3000	200	1800	20	50	1.0	0.5	0.16
37	250	25	2600	20	50	1.0	0.5	0.19
38	3000	25	2600	20	50	1.0	0.5	0.06
39	250	200	2600	20	50	1.0	0.5	0.54
40	3000	200	2600	20	50	1.0	0.5	0.16
41	250	25	1800	80	50	1.0	0.5	0.38
42	3000	25	1800	80	50	1.0	0.5	0.12
43	250	200	1800	80	50	1.0	0.5	1.07
44	3000	200	1800	80	50	1.0	0.5	0.31
45	250	25	2600	80	50	1.0	0.5	0.38
46	3000	25	2600	80	50	1.0	0.5	0.12
47	250	200	2600	80	50	1.0	0.5	1.07
48	3000	200	2600	80	50	1.0	0.5	0.31
49	250	25	1800	20	300	1.0	0.5	0.46
50	3000	25	1800	20	300	1.0	0.5	0.13
51	250	200	1800	20	300	1.0	0.5	1.31
52	3000	200	1800	20	300	1.0	0.5	0.38
53	250	25	2600	20	300	1.0	0.5	0.47
54	3000	25	2600	20	300	1.0	0.5	0.13
55	250	200	2600	20	300	1.0	0.5	1.31
56	3000	200	2600	20	300	1.0	0.5	0.38
57	250	25	1800	80	300	1.0	0.5	0.93
58	3000	25	1800	80	300	1.0	0.5	0.27
59	250	200	1800	80	300	1.0	0.5	2.63
60	3000	200	1800	80	300	1.0	0.5	0.76
61	250	25	2600	80	300	1.0	0.5	3.82
62	3000	25	2600	80	300	1.0	0.5	1.10
63	250	200	2600	80	300	1.0	0.5	2.63
64	3000	200	2600	80	300	1.0	0.5	0.76
65	250	25	1800	20	50	0.5	∞	0.13
66	3000	25	1800	20	50	0.5	∞	0.04
67	250	200	1800	20	50	0.5	∞	0.38
68	3000	200	1800	20	50	0.5	∞	0.11
69	250	25	2600	20	50	0.5	∞	0.13
70	3000	25	2600	20	50	0.5	∞	0.04
71	250	200	2600	20	50	0.5	∞	0.38
72	3000	200	2600	20	50	0.5	∞	0.11
73	250	25	1800	80	50	0.5	∞	0.27
74	3000	25	1800	80	50	0.5	∞	0.09
75	250	200	1800	80	50	0.5	∞	0.76

Table 2 *(continued)*

Row No.	Yield stress Pa	Plastic viscosity Pa s	Density kg/m^3	Poker diameter mm	Frequency Hz	Amplitude mm	Container size[a] m	Predicted radius of action m
76	3000	200	1800	80	50	0.5	∞	0.22
77	250	25	2600	80	50	0.5	∞	0.27
78	3000	25	2600	80	50	0.5	∞	0.09
79	250	200	2600	80	50	0.5	∞	0.76
80	3000	200	2600	80	50	0.5	∞	0.22
81	250	25	1800	20	300	0.5	∞	0.33
82	3000	25	1800	20	300	0.5	∞	0.1
83	250	200	1800	20	300	0.5	∞	0.93
84	3000	200	1800	20	300	0.5	∞	0.27
85	250	25	2600	20	300	0.5	∞	0.33
86	3000	25	2600	20	300	0.5	∞	0.1
87	250	200	2600	20	300	0.5	∞	0.93
88	3000	200	2600	20	300	0.5	∞	0.27
89	250	25	1800	80	300	0.5	∞	0.66
90	3000	25	1800	80	300	0.5	∞	0.19
91	250	200	1800	80	300	0.5	∞	1.86
92	3000	200	1800	80	300	0.5	∞	0.54
93	250	25	2600	80	300	0.5	∞	0.66
94	3000	25	2600	80	300	0.5	∞	0.19
95	250	200	2600	80	300	0.5	∞	1.86
96	3000	200	2600	80	300	0.5	∞	0.54
97	250	25	1800	20	50	1.0	∞	0.19
98	3000	25	1800	20	50	1.0	∞	0.06
99	250	200	1800	20	50	1.0	∞	0.5
100	3000	200	1800	20	50	1.0	∞	0.16
101	250	25	2600	20	50	1.0	∞	0.19
102	3000	25	2600	20	50	1.0	∞	0.06
103	250	200	2600	20	50	1.0	∞	0.54
104	3000	200	2600	20	50	1.0	∞	0.16
105	250	25	1800	80	50	1.0	∞	0.38
106	3000	25	1800	80	50	1.0	∞	0.12
107	250	200	1800	80	50	1.0	∞	1.07
108	3000	200	1800	80	50	1.0	∞	0.31
109	250	25	2600	80	50	1.0	∞	0.38
110	3000	25	2600	80	50	1.0	∞	0.12
111	250	200	2600	80	50	1.0	∞	1.07
112	3000	200	2600	80	50	1.0	∞	0.31
113	250	25	1800	20	300	1.0	∞	0.46
114	3000	25	1800	20	300	1.0	∞	0.13
115	250	200	1800	20	300	1.0	∞	1.31
116	3000	200	1800	20	300	1.0	∞	0.38
117	250	25	2600	20	300	1.0	∞	0.47
118	3000	25	2600	20	300	1.0	∞	0.13
119	250	200	2600	20	300	1.0	∞	1.31
120	3000	200	2600	20	300	1.0	∞	0.38
121	250	25	1800	80	300	1.0	∞	0.93
122	3000	25	1800	80	300	1.0	∞	0.27
123	250	200	1800	80	300	1.0	∞	2.63
124	3000	200	1800	80	300	1.0	∞	0.76
125	250	25	2600	80	300	1.0	∞	0.93
126	3000	25	2600	80	300	1.0	∞	0.27
127	250	200	2600	80	300	1.0	∞	2.63
128	3000	200	2600	80	300	1.0	∞	0.76

[a] Free field conditions are denoted by the symbol ∞.

The principal effects identified in Table 2 are amplified graphically, with intermediate values to demonstrate the trends, in Figs. 8, 9 and 10. Fig. 8 shows the effect of poker diameter and frequency on the radius of action at a moderate yield stress of 1500 Pa with plastic viscosity from 25 to 250 Pa s. Fig. 9 shows the same at a moderate plastic viscosity of 100 Pa s with yield stress from 250 to 2500 Pa. These two graphs show the opposing effects of yield stress and plastic viscosity, which is shown more clearly in Fig. 10, which takes points at the approximate centre of the grids in Figs. 8 and 9. One point is omitted from Fig. 8 because the calculation became unstable. Points at high radius of action may be less certain because of the assumption that the radius at the interface is small compared to the wavelength.

The importance of the rheology of the fresh concrete being vibrated has not previously been quantified, although ordinary practical observation shows that workability is important. Two important issues emerge from Fig. 10. The first is that yield stress and plastic viscosity have opposite effects on the radius of action of a

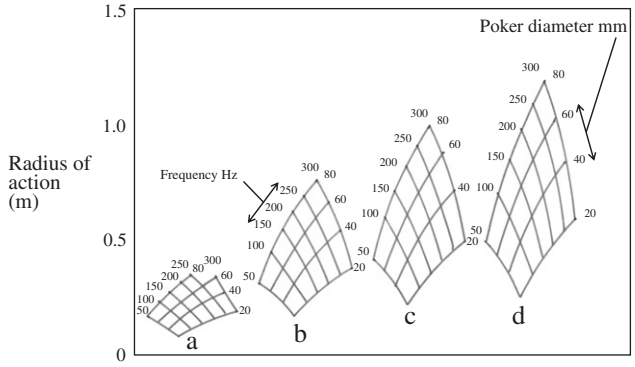

Fig. 8. Effect of poker diameter and frequency on the calculated radius of action in concrete of yield stress 1500 Pa, vibration amplitude 1.0 mm, concrete density 2400 kg/m^3. Plastic viscosity (a) 25 Pa s, (b) 100 Pa s, (c) 175 Pa s, (d) 250 Pa s.

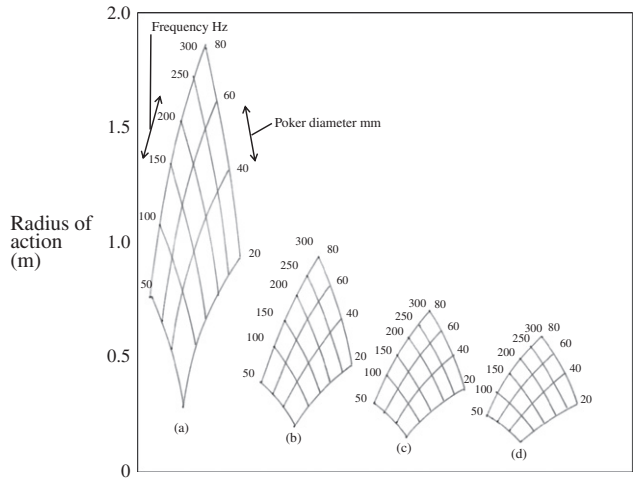

Fig. 9. Effect of poker diameter and frequency on the calculated radius of action in concrete of plastic viscosity 100 Pa s, vibration amplitude 1.0 mm, concrete density 2400 kg/m^3. Yield stress (a) 250 Pa, (b) 1000 Pa, (c) 1750 Pa, (d) 2500 Pa.

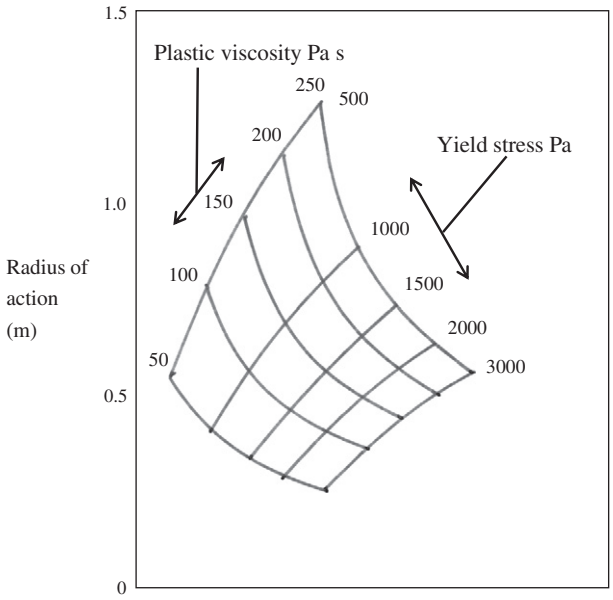

Fig. 10. Effect of yield stress and plastic viscosity on the calculated radius of action of a 50 mm diameter poker operating at frequency 75 Hz, amplitude 1.0 mm, in concrete of density 2400 kg/m^3.

given vibrator. This is a further reason for using two-point tests to characterise the concrete: a single point measurement (slump, flow, etc.), no matter how precise and sophisticated, cannot provide the necessary minimum of information, since an infinite number of combinations of yield stress and plastic viscosity can give the same single point result [2]. The second issue is that the combination of low yield stress and high plastic viscosity that gives the maximum radius of action (Fig. 10) is the same combination that is needed to ensure that concrete is self-compacting [19].

This work has not studied the rate of compaction. Since the viscosity of the vibrated concrete is proportional to the plastic viscosity of the unvibrated concrete [5] the flow and release of air bubbles during compaction is slower with higher plastic viscosities. However, the results presented here show that a high radius of action requires a high plastic viscosity so the productivity in practice is a compromise between the two requirements. A low plastic viscosity permits rapid compaction but the small radius of action requires the vibrator to be inserted many times at close spacing in the form, while a high plastic viscosity requires the vibrator to be held in one place for longer but without so many insertions.

8. Conclusions

An analysis of the compaction of fresh concrete by an internal poker vibrator has been developed using closed-form solutions for the shear and compressive waveforms based on the assumption that concrete conforms to the Bingham model. Theory and experiment agree well.

There are two distinct regions around the vibrating source. Near the vibrator the flow is controlled by the shear waveform and hydrodynamic theory may be used in the analysis, whereas outside this region the material is solid and the motion is governed by the compressive waveforms which can be solved by structural vibration theory.

The rapid decay of energy near the internal vibrator is due to the liquefaction and flow of the Bingham material and Dessoff's equation for estimating the radial distribution of vibrational energy is restricted to the case of the solid material outside the liquefied zone and cannot be used to predict the size of that zone.

The analysis developed in this study gives a method of predicting the radial position of the interface between the liquid and solid regions, i.e. the radius of action of the vibrator, as a function of the characteristics of the vibration and the rheology of the concrete. The radius of action increases with increasing plastic viscosity but decreases with increasing yield stress, with the optimum combination predicted to be a low yield stress with a high plastic viscosity. The work confirms the importance of velocity as the most important characteristic of the vibration governing efficacy. This work offers the potential to optimise the design and use of internal vibrators to achieve the most efficient and productive compaction of a concrete during production of constructional elements.

Acknowledgements

We are grateful to Alastair MacFarlane for technical assistance and development of the apparatus and to Vibratechniques Ltd, Brighton, UK and Tarmac Precast Concrete Ltd, Tallington, UK, for their technical support and advice. The work was supported financially by the Engineering and Physical Sciences Research Council, grant number GR/L52819/01.

References

[1] ACI Committee 309, Report on Behaviour of Fresh Concrete During Vibration, American Concrete Institute, Detroit, 2008 ACI 309.1R-08.
[2] G.H. Tattersall, P.F.G. Banfill, The Rheology of Fresh Concrete, Pitman, London, 1983 Out of print, but available as a CD-ROM from p.f.g.banfill@hw.ac.uk.
[3] G.H. Tattersall, P.H. Baker, The effect of vibration on the rheological properties of fresh concrete, Magazine of Concrete Research 40 (1988) 79–89.
[4] G.H. Tattersall, P.H. Baker, An investigation into the effect of vibration on the workability of fresh concrete using a vertical pipe apparatus, Magazine of Concrete Research 41 (1989) 3–9.
[5] P.F.G. Banfill, Xu Yongmo, P.L.J. Domone, Relationship between the rheology of unvibrated fresh concrete and its flow under vibration in a vertical pipe apparatus, Magazine of Concrete Research 51 (1999) 181–190.
[6] S. Ersoy, Untersuchungen uber die Verdichtungswirkung von Tauchruttler, Technische Hochschule, Aachen, 1962.
[7] L. Forssblad, Investigations of Internal Vibration of Concrete, Acta Polytechnica Scandinavica, Civil Engineering and Building Construction Series, 29, 1965 Stockholm.
[8] W.G. Goldstein, Wybor Parametrow Glubinnych Vibratorow dla Uplotnienia Betona, Moscow, , 1968.
[9] R.W. Taylor, The Compaction Of Concrete By Internal Vibrators – An Investigation Of The Effects Of Frequency And Amplitude Technical Report No 42.511, Cement and Concrete Association, Slough, 1976.
[10] M. Dessoff, Sur l'étude de la pervibration du béton, Annales des Ponts et Chaussées 5 (1937) 681–688.

[11] M.A.O.M. Teixeira, R.J.M. Craik, P.F.G. Banfill, Vibrational processing of fresh concrete: predicting fluidification from rheological behaviour, Proc. 13th International Congress on Rheology, 4, 2000, pp. 133–135.
[12] A.M. Alexander, Study of vibration in concrete, US Army Engineer Waterways Experiment Station, Vicksburg, 1977 Technical Report No. 6–780.
[13] S.S. Chen, M.W. Wambsganss, J.A. Jendrzejczyk, Added Mass and Damping of a Vibrating Rod in Confined Viscous Fluids, Transactions of the ASME, Journal of Applied Mechanics (June 1976) 325–329.
[14] H. Schlichting, Boundary Layer Theory, McGraw-Hill Inc., New York, 1960.
[15] P.M. Morse, K.U. Ingard, Theoretical Acoustics, McGraw-Hill Inc., New York, 1968.
[16] P.L.J. Domone, Xu Yongmo, P.F.G. Banfill, Developments of the two-point workability test for high-performance concrete, Magazine of Concrete Research 51 (1999) 171–180.
[17] BS EN 12350–6:2009, Testing fresh concrete, Density, British Standards Institution, 2009.
[18] R.B.J. Casson, P.L.J. Domone, K. Scrivener, H.M. Jennings, C.J. Gillham, P.L. Pratt, The use of ultrasonic pulse velocity, penetration resistance and electron microscopy to study the rheology of fresh concrete, in: J. Skalny (Ed.), Concrete Rheology, Proceedings of Symposium M, Materials Research Society, 1982, pp. 66–75.
[19] O.H. Wallevik, J.E. Wallevik, Rheology as a tool in concrete science: The use of rheographs and workability boxes, Cem. Concr. Res. (2011), doi:10.1016/j.cemconres.2011.01.009.